

Sulforaphane, a Naturally Occurring Isothiocyanate, Induces Cell Cycle Arrest and Apoptosis in HT29 Human Colon Cancer Cells

Laurence Gamet-Payrastre,¹ Pengfei Li, Solange Lumeau, Georges Cassar, Marie-Ange Dupont, Sylvie Chevallieu, Nicole Gasc, Jacques Tulliez, and François Tercé

INRA, Laboratoire des Xénobiotiques, 31931 Toulouse Cedex, France [L. G.-P., P. L., S. L., S. C., N. G., J. T.J.]; INSERM U326, 31059 Toulouse Cedex, France [F. T.]; INSERM U395, Service Commun d'Analyse et de Tri Cellulaire, 31024, Toulouse Cedex, France [G. C.]; and Laboratoire de Biologie Moléculaire des Eucaryotes, 31062, Toulouse Cedex, France [A. D., M.-A. D.]

ABSTRACT

Sulforaphane is an isothiocyanate that is present naturally in widely consumed vegetables and has a particularly high concentration in broccoli. This compound has been shown to block the formation of tumors initiated by chemicals in the rat. Although sulforaphane has been proposed to modulate the metabolism of carcinogens, its mechanism of action remains poorly understood. We have previously demonstrated that sulforaphane inhibits the reinitiation of growth and decreases the cellular viability of quiescent human colon carcinoma cells (HT29). Moreover, the weak effect observed on differentiated CaCo2 cells suggests a specific anticancer activity for this compound.

Here we investigated the effect of sulforaphane on the growth and viability of HT29 cells during their exponentially growing phase. We observed that sulforaphane induced a cell cycle arrest in a dose-dependent manner, followed by cell death. This sulforaphane-induced cell cycle arrest was correlated with an increased expression of cyclins A and B1. Moreover, we clearly demonstrated that sulforaphane induced cell death via an apoptotic process. Indeed, a large proportion of treated cells display the following: (a) translocation of phosphatidylserine from the inner layer to the outer layer of the plasma membrane; (b) typical chromatin condensation; and (c) ultrastructural modifications related to apoptotic cell death. We also showed that the expression of p53 was not changed in sulforaphane-treated cells. In contrast, whereas bcl-2 was not detected, we observed increased expression of the proapoptotic protein bax, the release of cytochrome c from the mitochondria to the cytosol, and the proteolytic cleavage of poly(ADP-ribose) polymerase. In conclusion, our results strongly suggest that in addition to the activation of detoxifying enzymes, induction of apoptosis is also involved in the sulforaphane-associated chemoprevention of cancer.

INTRODUCTION

The incidence of high disease with poor prognosis in humans, as is the case for colon cancer, is inversely correlated with the consumption of fruits and vegetables (1). The anticarcinogenic activities of isothiocyanates, a family of compounds found in large amounts in cruciferous vegetables in the form of the thioglucoside precursors (glucosinolates), have been demonstrated in rodents treated with a wide variety of chemical carcinogens. Moreover, these compounds exhibit a protective effect against cancer in a variety of target organs such as lung, esophagus, mammary gland, liver, small intestine, colon, and bladder (2). Most isothiocyanates have shown chemopreventive activity in protocols involving their administration either before or during exposure to the carcinogen (3).

The mechanisms by which isothiocyanates might exert their anticarcinogenic effects remain unclear. One proposed hypothesis involves the modulation of the metabolism of carcinogens (4, 5). The fate of chemical carcinogens *in vivo* is determined at least in part by the balance between phase I and phase II enzymes: phase I enzymes

activate many carcinogens to highly reactive electrophilic metabolites capable of damaging DNA; phase II enzymes convert these reactive electrophiles to less toxic and more easily excreted products. It has been hypothesized that isothiocyanates may competitively inhibit enzymes such as cytochrome P-450 involved in the bioactivation of carcinogens (5). The chemopreventive properties of isothiocyanates are also associated with the induction of phase II detoxifying enzymes including glutathione S-transferase, quinone reductase, epoxide hydrolase, and UDP-glucuronosyltransferase. Indeed, molecular studies have shown that isothiocyanates can induce phase II enzymes by stimulating transcription of their genes via a common antioxidant/electrophile enhancer element present in the upstream region of several phase II enzyme genes (5, 6).

However, some recent results suggest that the chemopreventive activities of isothiocyanates may involve other mechanisms as well. Indeed, isothiocyanates could also act at the DNA level or affect signal transduction pathways leading to growth arrest or cell death. Stoner *et al.* (7) have established that the inhibitory effects of PEITC² on the production of esophagus tumors by *N*-nitrosobenzylmethylamine in rats paralleled the inhibition of the binding of the carcinogen to DNA and the formation of *N*-methylguanine and (*O*)-methylguanine. In addition, it was recently reported that PEITC could induce *in vitro* activation of c-Jun NH₂-terminal kinase 1, an activation associated with the induction of apoptosis (8). Moreover Huang *et al.* (9) have demonstrated that PEITC also induces p53 transactivation in a dose-and time-dependent fashion, a mechanism required for the PEITC-induced apoptosis and antitumor promotion effects of this compound in mouse epidermal cells.

Sulforaphane is an isothiocyanate that has been isolated from SAGA broccoli as the major phase II enzyme inducer present in organic solvent extracts of this vegetable (10). Our interest on sulforaphane stemmed from the following observations: (a) it occurs naturally in widely consumed vegetables and at a particularly high concentration in broccoli (11); (b) it blocks chemical-initiated tumor formation in rats (11); (c) it is a very potent monofunctional inducer of phase II enzymes in both cultured cells and mouse tissues; and (d) it has recently been shown to inhibit at least one cytochrome P-450 (CYP2E1) involved in the activation of a variety of carcinogens (11, 12).

In this study, we have investigated whether sulforaphane has direct anticancer activities besides its blocking action on carcinogenesis. In a previous study (13), we have shown that sulforaphane inhibits the reinitiation of growth and diminishes cellular viability in quiescent colon carcinoma cells (HT29) and had a lower toxicity on differentiated CaCo2 cells.

Here we show that in highly proliferative HT29 cells, sulforaphane induces a cell cycle arrest, followed by cell death. This arrest is correlated with an increased expression of cyclins A and B1. Moreover, we clearly demonstrate that sulforaphane induces cell death

Received 7/13/99; accepted 1/6/00.

The costs of publication of this article were defrayed in part by the payment of page charges. This article must therefore be hereby marked *advertisement* in accordance with 18 U.S.C. Section 1734 solely to indicate this fact.

¹ To whom requests for reprints should be addressed, at INRA, Laboratoire des Xénobiotiques, 180 Chemin de Tournefeuille BP 3, 31931 Toulouse, Cedex 9, France.

² The abbreviations used are: PEITC, phenylethyl isothiocyanate; PARP, poly(ADP-ribose) polymerase; PI, propidium iodide; PS, phosphatidylserine; MTT, 3-(4,5-dimethylthiazol-2-yl)-2,5-diphenyltetrazolium bromide; cdk, cyclin-dependent kinase.

through an apoptotic pathway involving typical biochemical and ultrastructural modifications related to programmed cell death. We also demonstrate that the activation of the proapoptotic protein bax, but not p53, is required for sulforaphane-induced cell death. Finally, bax induction is correlated with cytochrome *c* release from the mitochondria to the cytosol and PARP cleavage. Our results strongly suggest that in addition to the activation of detoxifying enzyme activities, specific mechanisms such as apoptosis are also involved in the sulforaphane-associated chemoprevention of cancer.

MATERIALS AND METHODS

Drugs and Chemicals

DMEM and FCS were purchased from Life Technologies, Inc. Annexin V-fluorescein was obtained from Boehringer Mannheim (France). Antibody to bcl-2 was obtained from Santa Cruz Biotechnology, and antibodies to actin, p53, PARP, bax, and cyclins A and B1 were purchased from Pharmingen (Le Pont de Claix, France). Peroxidase-labeled rabbit antimouse immunoglobulin was purchased from Sigma (St. Louis, MO). [³H]Thymidine, [³H]uridine, [³H]choline, and [³H]leucine were from Amersham. All other chemicals were purchased from Sigma or Merck and were of the highest purity available. Sulforaphane was synthesized according to the method described by Schmid and Karrer (14), with slight modifications. The product was purified just before use by high-performance liquid chromatography (Hewlett Packard System Series 1050) on a reverse-phase column [Ultrabase C18 (250 × 4.6 mm)] using elution, starting with 100% solution A (20% acetonitrile, 80% H₂O, v/v) for 10 min, followed by a 10-min linear gradient to reach 100% solution B (90% acetonitrile, 10% H₂O, v/v). Sulforaphane elution buffers were detected at 245 nm; the product was collected, dried under nitrogen, and then dissolved in ethanol at a concentration of 30 mM and stored at -20°C.

Cell Culture

The HT29 cell line was established in permanent culture from a human colon carcinoma by Dr. J. N. Fogh (Sloan Kettering Institute for Cancer Research, Rye, NY; Ref. 15). HT29 cells were purchased from European Collection of Cell Culture (Salisbury, United Kingdom). Stock cells were routinely cultured in DMEM containing 25 mM glucose, 43 mM bicarbonate, 60 µM/ml penicillin, and 100 µg/ml streptomycin at 37°C under an air:CO₂ (9:1) atmosphere supplemented with 5% heat-inactivated FCS, and the medium was changed every 48 h. For the experiments, HT29 cells were seeded at low density (5 × 10⁴ cells/ml) in 35- or 120-mm diameter Primaria dishes in standard medium containing 5% FCS. One day after seeding, medium was changed, and HT29 cells were treated with sulforaphane. An equivalent amount of the solvent (ethanol) was added to control cells (0.2% final concentration).

Cell Viability Assay

Drug effect on cellular viability was evaluated using an assay based on the cleavage of the yellow dye MTT to purple formazan crystals by dehydrogenase activity in mitochondria, a conversion that occurs only in living cells (16). At each time point, cells were rinsed with phenol red-free RPMI 1640, and then they received MTT diluted in RPMI 1640 for 4 h. The cells were then solubilized in SDS/NaOH, and the optical density of the cellular homogenate was measured at 570 and 690 nm.

Flow Cytometry Analysis

Drug effect on cell proliferation was evaluated by measuring the distribution of the cells in the different phases of the cell cycle by flow cytometry. This determination was based on the measurement of the DNA content of nuclei labeled with propidium iodide according to the method of Vindelov and Christensen (17), with slight modifications. Cell suspensions from either

control cultures or treated cultures were prepared by trypsinization and washed twice with 0.9% NaCl. Cells (1 × 10⁶) were resuspended in 220 µl of solution A (3.4 mM trisodium citrate (pH 7.6), 0.1% NP40, 1.5 mM spermine tetrahydrochloride, and 0.5 mM Trisbase containing trypsin (30 mg/liter) for 10 min at room temperature. Trypsin was then inhibited by the addition of 180 µl of solution A containing trypsin inhibitor (0.5 g/liter) and RNase A (100 mg/liter) for an additional 10 min. Finally, nuclei were labeled by the addition of 180 µl of solution A containing PI (416 mg/liter) and additional spermine tetrahydrochloride (1160 mg/liter). The suspension was incubated overnight at 4°C to allow maximum labeling of DNA. Cell cycle analysis was performed on a Coulter ELITE flow cytometer through a 630 nm LP filter. Debris and doublets were eliminated by gating on peak *versus* integrated signals, and 1.5 × 10⁴ cells were collected per sample. Calculations were performed with MULTICYCLE AV Software (Phoenix Flow System).

Determination of Apoptosis

Analysis of Chromatin Condensation. Cells were plated at low density (1.25 × 10⁵ cells/well) on glass coverslides (Esco; 20 × 20 mm; Erie Scientific, Portsmouth, NH) in a 6-well plate and treated with sulforaphane for 48 h. At the end of the experiment, cells were washed twice with PBS at room temperature and then fixed with ice-cold methanol/ethanol (v/v, 1/1) for 10 min at -20°C. Fixed cells were rinsed with PBS and stained with Hoechst 33342 (10 µg/ml) in PBS (15 min at room temperature in the dark). Finally, cells were washed three times with PBS and analyzed under a fluorescence microscope with a UV light filter.

Detection of PS on the Outer Leaflet of Cells. Analysis of the presence of PS on the outer leaflet of cell membrane was performed using a double-labeling experiment with annexin V-fluorescein and PI to discriminate apoptotic from necrotic cells. In the presence of calcium, annexin V binds to PS, which are translocated to the outer leaflet of the plasma membrane of apoptotic cells. PI is a nonpermeant cell marker that is able to label the DNA of cells with a permeable plasma membrane, *i.e.*, necrotic or lysed cells. Cells that stain only for annexin V are considered apoptotic.

Cells were plated and treated as described above. After washing twice with PBS and once with the incubation buffer [10 mM HEPES/NaOH (pH 7.4), 140 mM NaCl, and 5 mM CaCl₂], cells were incubated with annexin V-fluorescein and PI (1 µg/ml) for 10 min in the dark at room temperature. Cells were then washed two times with the incubation medium and fixed for 10 min in an ice-cold solution of methanol/ethanol (v/v, 1/1) at -20°C. Analysis was performed on a fluorescence microscope (488 nm excitation and a 515 nm longpass filter for detection).

Electron Microscopy Analysis. HT29 cells were plated at a density of 7.5 × 10⁵ cells/flask (Nunc, 80 cm²) and treated with control (ethanol) or sulforaphane-supplemented medium for 24, 48, or 72 h. At the end of each incubation time, cells were fixed for 2 h with 3% glutaraldehyde in 0.1 M sodium cacodylate buffer (fixation buffer). After three washes in the same buffer, cells were postfixed with 1% osmium tetroxide and then dehydrated in graded ethanol. The 100% ethanol solution was then replaced by propylene oxide and embedded in epon 812. Sections were stained with uranyl acetate and lead citrate and then examined with a Jeol 1200EX electron microscope.

For light microscopy observations, the epon-embedded semithin sections were stained with 1% methylene blue/azur II (v/v) for 10 min, rinsed with water, and observed using a Leitz Ortholux II microscope.

Measurement of DNA, RNA, Protein, and Phospholipid Synthesis

[³H]Thymidine (59 Ci/mmol), [³H]leucine (60 Ci/mmol), [³H]uridine (25 Ci/mmol), and [³H]choline (85 Ci/mmol) were used as markers for the biosynthesis of DNA, protein, RNA, and the major phospholipid phosphatidylcholine, respectively, as follows: cells were seeded at 5 × 10⁵ cells/ml for 1 day, and then each marker (1 µCi/ml) was added independently to the culture medium together with ethanol (control) or sulforaphane (15 µM). At each time point, cells were washed twice with ice-cold PBS, treated with 10% ice-cold trichloroacetic acid (15 min on ice), and washed twice with 10% trichloroacetic acid to remove unincorporated label. The precipitate was then dissolved in 0.1 N NaOH and 0.1% SDS for 4 h at room temperature. Aliquots were counted in a Packard B counter in the presence of Ultimagold scintillation liquid. All experiments were carried out in triplicate.

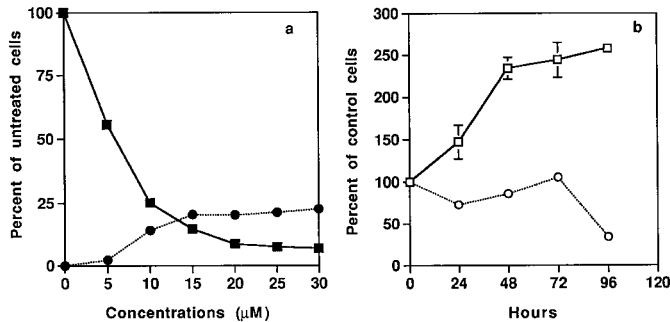


Fig. 1. Effect of sulforaphane on HT29 cell growth and viability. *a*, 1 day after seeding, cells were treated with increasing concentrations of sulforaphane for 48 h. At the end of the incubation, the number of cells present in the culture medium (●) that adhered to the plate (■) was determined. Results are expressed as the percentage of untreated cells. *b*, cell viability in control (□) or in 15 μ M sulforaphane-treated cells (○) was measured every day using the MTT assay as described in "Materials and Methods." Results are expressed as the percentage of viable cells at the beginning of the experiment (time 0) and are the mean \pm SE of four separate experiments. When they do not appear, error bars are smaller than the symbol size.

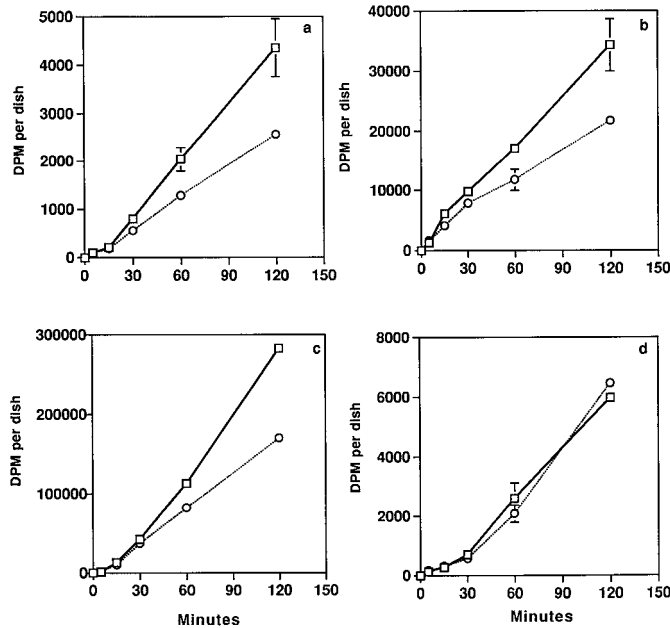


Fig. 2. Effect of sulforaphane on DNA (*a*), protein (*b*), RNA (*c*), and phospholipid (*d*) synthesis in HT29 cells. One day after seeding, cells were treated with 0 (□) or 15 (○) μ M sulforaphane in the presence of 1 μ Ci of either [³H]thymidine (*a*), [³H]leucine (*b*), [³H]uridine (*c*), or [³H]choline (*d*). At the indicated time, the radioactivity incorporated in the respective fractions was measured as described in "Materials and Methods." Results are expressed as dpm/dish and are the mean \pm SE of four separate experiments. The difference between control and treated cells was significant for *a-c*.

Determination of Intracellular ATP Content

Intracellular ATP levels were determined by capillary zone electrophoresis according to the method of Kamaryt *et al.* (18), with slight modifications.

Cells were scraped in 0.6 M perchloric acid, and homogenates were rapidly neutralized with 0.75 M K₂CO₃ and centrifuged at 14,000 rpm for 1 min. The neutralized supernatants were filtered through 0.45- μ m membrane filters before analysis. ATP standard solutions (concentrations between 7.81 and 125 μ M) were prepared in a mixture of 0.6 M HClO₄ 0.75 M K₂CO₃ (3.5:1.4, v/v) and filtered through 0.45- μ m membrane filters.

Capillary zone electrophoresis was carried out on a HP ^{3D}CE System (Hewlett-Packard Co., Wilmington, DE) with a built-in UV diode-array detector. Capillary zone electrophoresis separations were performed using a noncoated fused silica capillary equipped with a bubble detection cell to improve detection sensitivity (68.5 cm \times 50/150 μ m inner diameter; 60 cm, effective length; Hewlett Packard). Experiments were carried out in the cationic mode by applying a voltage of 30 kV. Hydrostatic injection was applied

for 6 s at 50 mbar, followed by a 3-s flush with the buffer. Detection wavelength was 260 nm. The temperature was kept constant at 25°C. To improve the migration time and peak shape reproducibility, the system was rinsed between each run as follows: 3 min with 0.1 M NaOH, followed by 5 min with running buffer 50 mM disodium tetraborate (pH 9.18).

The detector response linearity over the range has been determined (correlation coefficient, 0.99949). Ten preparations of ATP standard (125 μ mol/liter) have been analyzed to determine the repeatability of the analysis (Relative Standard Deviation = 2.14%). The lower limit of detection was about 2 μ mol/liter ATP (signal:noise ratio = 3).

Western Blot Analysis

The levels of p53, bax, cytochrome *c*, cyclin B1, cyclin A, and actin were measured by Western blotting with specific antibodies against these proteins. Cells (5×10^5) were seeded in Primaria dishes. One day later, cells were treated without or with 15 μ M sulforaphane for 24 h and then trypsinized, washed with ice-cold PBS, and counted. For bax, p53, and cyclin analysis,

Table 1 Intracellular content of ATP in control (untreated) and sulforaphane-treated cells

At the indicated times, cells were harvested in perchloric acid, rapidly neutralized, and centrifuged as indicated in "Materials and Methods." The neutralized supernatant was then analyzed by capillary zone electrophoresis, and ATP content was calculated according to ATP standard solutions. The differences between control and treated cells are not significant at any time point (Student's *t* test).

	ATP (10^{-9} M/dish)			
	0.5 h	1 h	3 h	8 h
Control	6.85 \pm 0.15	7.31 \pm 0.16	8.25 \pm 0.18	10.75 \pm 0.23
15 μ M sulforaphane	5.95 \pm 0.13	7.05 \pm 0.15	8.80 \pm 0.19	11.45 \pm 0.24

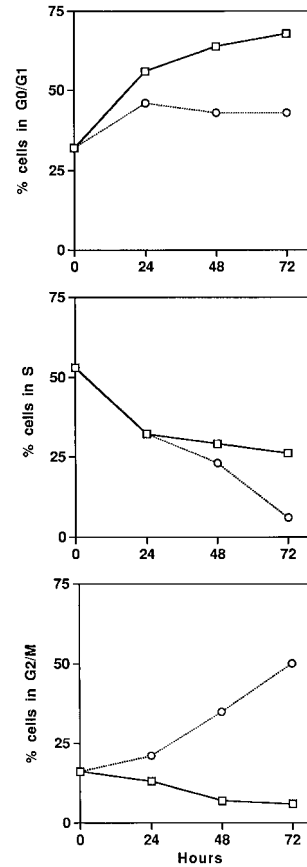


Fig. 3. Effect of sulforaphane on HT29 cell cycle distribution. One day after seeding, cells were treated with 0 (□) or 15 (○) μ M sulforaphane for up to 3 days. At the indicated time, distribution of the cells in G₀-G₁, S phase, and G₂-M phase was analyzed by flow cytometry as described in "Materials and Methods." Results are expressed as the percent age of total cells and are from one typical experiment among five experiments.

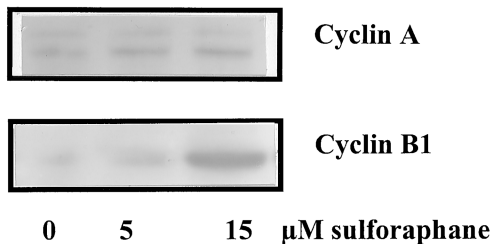


Fig. 4. Western blots of cyclin A and B1 in sulforaphane-treated cells. One day after seeding, HT29 cells were treated with 0 (control cells), 5, or 15 μM sulforaphane for 24 h. Cellular lysates (from 2×10^5 cells) were prepared as described in "Materials and Methods" and fractionated on 7.5% SDS-PAGE gels. Cyclins A and B were analyzed by Western blotting.

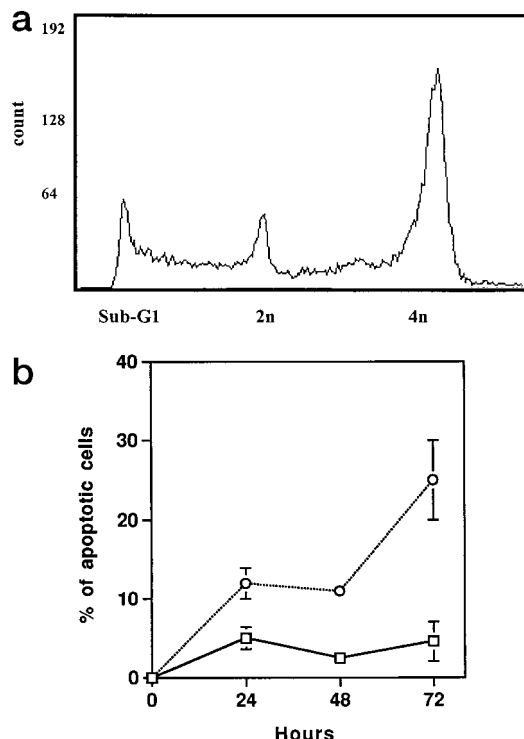


Fig. 5. Flow cytometry analysis of sulforaphane-treated cells. Cells were incubated for different times with ethanol [control (□)] or 15 μM sulforaphane (○). At the indicated times, total cells were treated as described in "Materials and Methods," and DNA content was analyzed by flow cytometry. *a*, typical flow cytometry pattern indicates the presence of sub-G₁ cells (apoptotic). *b*, the percentage of sub-G₁ peak cells was calculated for each time point. Results are the mean \pm SE of three separate experiments.

2×10^5 cells were lysed on ice in 62.5 mM Tris (pH 6.8) containing 2% SDS, 5% glycerol, and 2.5% 2-mercaptoethanol (lysis buffer).

For cytochrome *c* and actin determination, 5×10^7 cells were suspended in 5 volumes of 20 mM HEPES (pH 7.5), 10 mM KCl, 1.5 mM MgCl₂, 1 mM EDTA, 1 mM EGTA, 1 mM DTT, 0.1 mM phenylmethylsulfonyl fluoride, and 10 μM leupeptin containing 20 mM sucrose. After chilling on ice for 30 min, the cells were disrupted by stroking 40 times in a glass homogenizer. The nuclei were centrifuged at $1,000 \times g$ for 10 min at 4°C. The resulting supernatant was centrifuged at $10,000 \times g$ for 30 min to pellet mitochondria. A final centrifugation at $100,000 \times g$ for 1 h at 4°C generated the cytoplasmic fraction.

Cell extracts or subfractions were then mixed with loading buffer 250 mM Tris (pH 8.8), 4% SDS, 16% glycerol, 8% 2-mercaptoethanol, and 0.1% bromophenol blue; fractionated by electrophoresis on SDS-polyacrylamide gels (7.5% for p53 and cyclin A and B, 14% for bax, and cytochrome *c*); and transferred to nitrocellulose membranes (Schleicher & Schuell, Keene, NH) by electroblotting. After transfer, the filters were incubated in saturating buffer (137 mM NaCl, 2.7 mM KCl, 4.3 mM Na₂HPO₄ · 2H₂O, 1.4 mM KH₂PO₄,

0.05% Tween 20, and 3% nonfat dry milk) at 4°C overnight. Blots were subsequently incubated for 1.5 h at room temperature with the desired primary antibodies. After rinsing with saturating buffer, the filters were incubated with diluted enzyme-linked secondary antibody for 1.5 h. The proteins were then visualized with an enhanced chemiluminescence detection system (Pierce) according to the manufacturer's instructions.

Statistical Method

Statistical calculations were done using Student's *t* test.

RESULTS

Cytotoxicity of Sulforaphane on Colon Cancer Cell Growth. In a previous work (13), we have shown that sulforaphane, ranging from 5 to 50 μM , inhibited FCS-induced cell growth and promoted cell death of synchronized quiescent HT29 cells in a dose-dependent manner. In this study, we investigated the effect of sulforaphane on nonsynchronized HT29 cells. When HT29 cells were incubated for 48 h with increasing concentrations of sulforaphane, we observed a net decrease in the total number of cells and an accumulation of cells floating in the culture medium (Fig. 1*a*). The inhibition of growth and

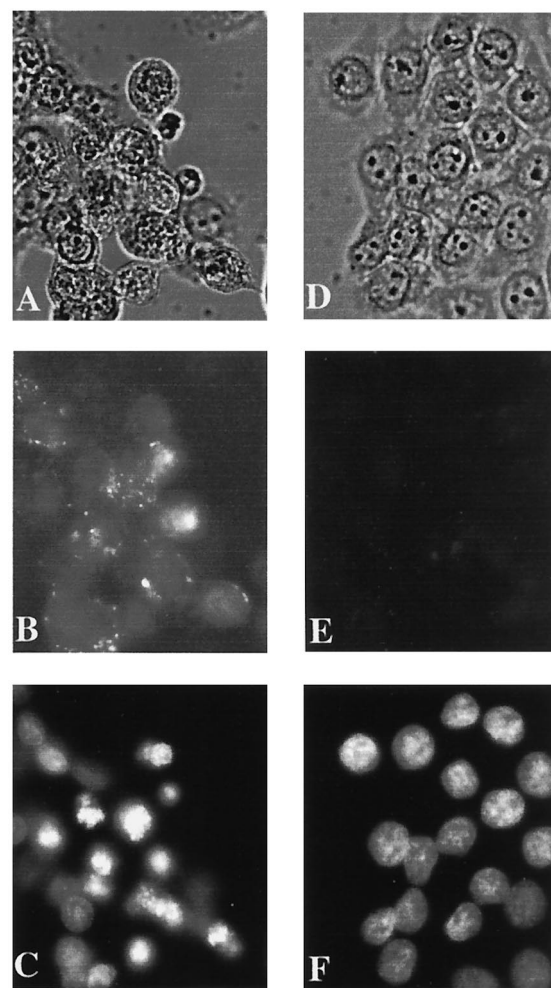


Fig. 6. Sulforaphane induces condensation of nuclear chromatin and PS translocation in HT29 cells. One day after seeding, HT29 cells were treated with 0 or 15 μM sulforaphane for 48 h, followed by fixation and staining with annexin V-fluorescein or Hoechst 33342 as described in "Materials and Methods." *A* and *D*, phase-contrast microscope analysis of sulforaphane-treated cells (*A*) and control cells (*D*); *B* and *E*, annexin V-fluorescein binding to PS exposed at the surface of treated cells (*B*) and not control cells (*E*). *C* and *F*, condensed nuclear chromatin in sulforaphane-treated cells (*C*) compared with control cells (*F*) was demonstrated using Hoechst 33342 DNA staining as described in "Materials and Methods."

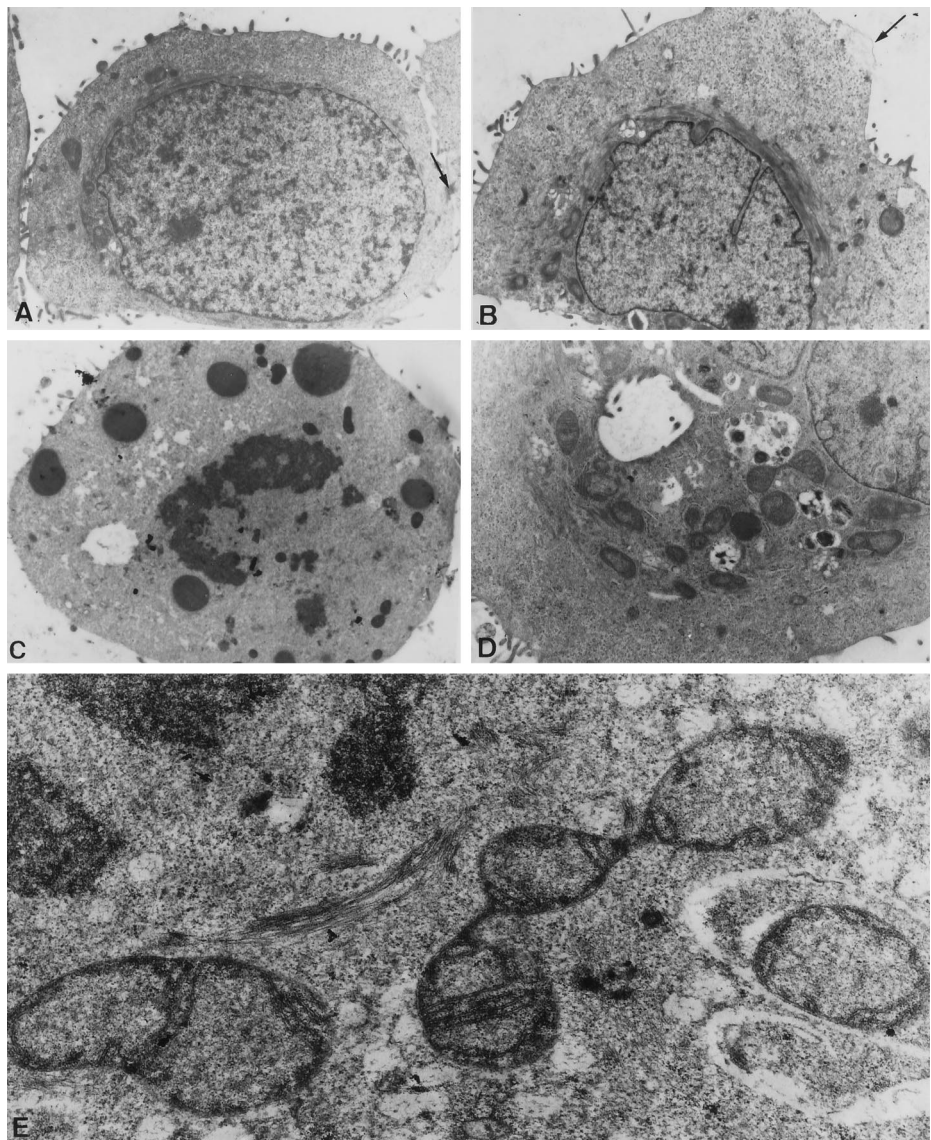


Fig. 7. Changes after 15 μM sulforaphane treatment in HT29 cells. One day after seeding, cells were treated with either 0 or 15 μM sulforaphane for 24 h and then fixed as described in "Materials and Methods." *A*, control cells with apparent desmosome (arrow) and microvilli. *B–F*, 24 h. Arrow in *B* shows membrane blebbing. *C*, compaction and margination of nuclear chromatin into an amorphous mass osmophilic is quite obvious after sulforaphane treatment. *D*, vesicle formation and abundant vacuole formation. Multivesicular bodies appear. *E*, mitochondrial changes can be characterized by the interruption and/or absence of the cristae and the loss of matrix density.

the effect on the adherence were already important at 15 μM (of the total cells present in the plate, 46% were attached and 62% were floating), thus this concentration was used in all further experiments. Viability was determined by using the MTT assay on cells treated with the drug for up to 96 h. As shown in Fig. 1*b*, sulforaphane at 15 μM was able to inhibit cell growth and induce cell death. Cell mortality was already 75% at 24 h and almost total at 96 h.

Treatment of HT29 Cells with Sulforaphane Results in a Decrease in DNA, RNA, Protein, and Phospholipid Synthesis. To determine which major biosynthetic pathway was primarily inhibited, the effect of sulforaphane on DNA, RNA, protein, and phospholipid synthesis was analyzed by measuring the incorporation of the respective markers [^3H]thymidine, [^3H]uridine, [^3H]leucine, and [^3H]choline. As shown in Fig. 2*a*, [^3H]thymidine incorporation into DNA was rapidly inhibited after sulforaphane treatment, decreasing to 63 \pm 4% of control levels within 60 min. Protein synthesis (Fig. 2*b*) and RNA (Fig. 2*c*) synthesis were also inhibited in a similar manner. In each case, the inhibitory effect of sulforaphane was maintained over a 24-h period of treatment (data not shown). However, the first significant inhibition (30%) was observed at 30 min for DNA synthesis, whereas 60 min were needed for RNA and protein synthesis. As estimated by [^3H]choline incorporation into phosphatidylcholine, the major class of

phospholipid (50% of total cellular phospholipids), phospholipid synthesis was not altered by sulforaphane at up to 2 h of treatment (Fig. 2*d*). However, it decreased dramatically (down to 47%) after 3 h of treatment, indicating that a prolonged treatment affects all the major biosynthetic pathways (data not shown).

Effect of Sulforaphane on ATP Levels. Because one common metabolite required for the major biosynthetic pathways is the energy donor ATP, we tried to measure the amount of ATP in cells treated with sulforaphane. As indicated in Table 1, no difference in ATP level could be seen after up to 8 h of incubation between control and treated cells, ruling out ATP as the initial trigger of the biochemical events.

Sulforaphane-treated HT29 Cells Are Blocked in G₂-M Phase of the Cell Cycle and Express High Levels of Cyclin A and B1. Cell cycle response of HT29 cells to sulforaphane was examined at various times (Fig. 3). At time 0, most cells (60%) were in S phase, due to the high proliferative state of this cell line. Untreated control cells showed the expected pattern for continuously growing cells. However, in the presence of 15 μM sulforaphane, we observed a net increase in the percentage of cells in the G₂-M phase of the cell cycle that was maintained throughout the overall time of treatment (3 days). These results suggest that the G₂-M phase accumulation was caused not only by an increase in the duration of the G₂-M phase, but by a

complete arrest of many cells in the G₂-M. The G₂-M-phase accumulation was accompanied by a decrease in the percentage of cells in S phase.

To investigate possible mechanisms by which sulforaphane would interfere with cell cycle progression, we evaluated the cellular content of G₂-M-phase-related cyclins A and B1. Fig. 4 shows that according to the blockage in the G₂-M phase, exponentially growing cells treated with 15 μ M sulforaphane expressed high levels of cyclin A and B1 as compared with control cells.

Sulforaphane Induces Apoptosis in HT29 Cells. Interestingly, flow cytometry analysis also showed the presence of a sub-G₁ peak characteristic of potential apoptotic cells (Fig. 5a). Indeed, the number of cells with subdiploid DNA content increased with time to reach 30% at 72 h (Fig. 5b). Moreover, about half of the floating cells recovered in the culture medium were subdiploid, with the other half being in the G₂-M phase (data not shown), strengthening the relationship between G₂-M-phase accumulation and apoptotic triggering. To confirm the existence of an apoptotic process, we have analyzed the presence of apoptosis by different techniques.

The classical DNA ladder assay shown by gel electrophoresis did not reveal an apoptotic pattern in HT29 cells treated with sulforaphane for up to 3 days (data not shown). However, the absence of DNA degradation in small fragments has also been reported in some cells undergoing apoptosis (19), and we cannot exclude the cleavage of DNA in a high molecular weight fragment undetectable by simple agarose gel electrophoresis.

Nuclear chromatin condensation is considered to be part of the cellular events involved in apoptosis. Therefore, we have analyzed the fluorescence of the nuclei of cells stained with the DNA-specific dye Hoechst 33342. Pictures were taken after 48 h of treatment (Fig. 6). In untreated cells, we observed normal nuclei staining (Fig. 6F). By contrast, sulforaphane-treated cells (15 μ M) displayed typical condensed chromatin and fragmented nuclei (Fig. 6C). In addition, the dying cells appeared rounded (Fig. 6A) compared to control cells (Fig. 6D) when observed using phase-contrast microscopy.

During apoptosis, one of the classical alterations observed at the plasma membrane level is the translocation of PS from the inner layer to the outer layer, exposing PS at the external surface of the cell. Annexin V is a calcium-dependent phospholipid-binding protein with high affinity for PS that can be used as a sensitive probe for PS exposure when linked to fluorescein. As shown in Fig. 6E, control cells did not show fluorescence staining. In contrast, treated cells displayed the binding of annexin V-fluorescein to the plasma membrane after 48 h of treatment (Fig. 6B). To distinguish between apoptotic and potential necrotic or lysed cells that may also expose PS according to the loss of membrane integrity, we have concomitantly used PI, a DNA dye that is excluded from cells with a nonleaky plasma membrane (*i.e.*, normal or apoptotic). We never observed PI staining among the annexin V-positive cells (data not shown), excluding the presence of necrotic or lysed cells in the population.

Morphological and ultrastructural changes of HT29 cells exposed to 15 μ M sulforaphane were examined at various times by electron microscopy (Fig. 7) or light microscopy (Fig. 8). In the healthy control cells (Figs. 7A and 8A), desmosomes keeping cells attached to each other in the organized cell monolayer were clearly seen (*arrow*). Moreover, the structure of the nucleus, as well as the size and shape of the mitochondria, was normal. In contrast, in treated cells, characteristics of apoptosis [namely, cell detachment, membrane blebbing (Fig. 8E), cell shrinkage with a condensed cytoplasm, and vesicle formation (abundant vacuoles with multivesicular bodies)] appeared (Fig. 7D). The compaction and margination of nuclear chromatin into an amorphous mass osmophilic is quite obvious (Fig. 7C and Fig. 8B-E). We also observed swelling of the endoplasmic reticulum

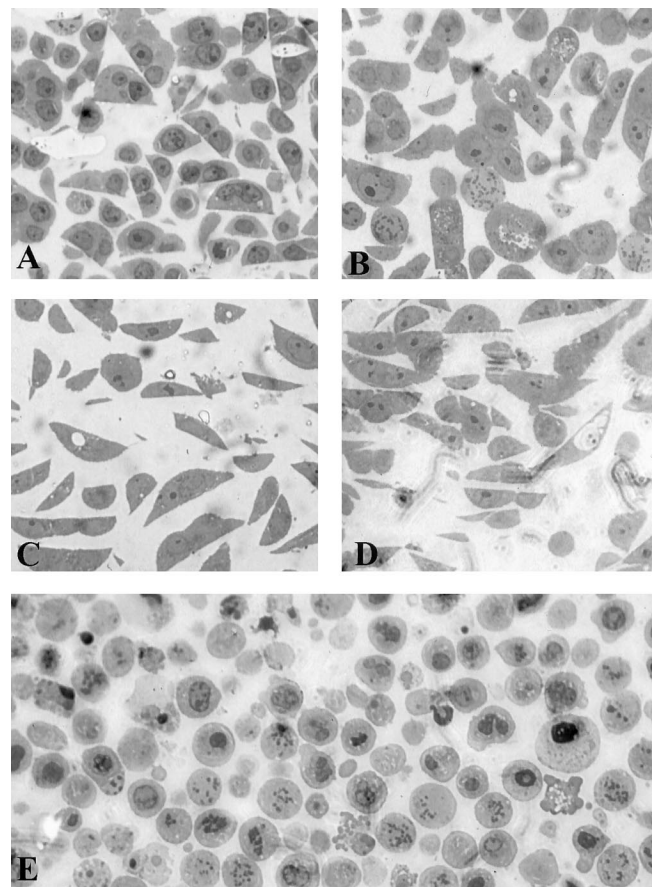


Fig. 8. Methylene blue staining and Azur II-stained semithin sections of control (A) and treated cells after 24 (B and E), 48 (C), and 72 (D) h. As early as 24 h, cells became round, and typical apoptotic changes are observed in sulforaphane-treated cells such as membrane blebbing and condensed nuclear chromatin (*arrow* on Fig. 9E).

cisternae (Fig. 7B). Moreover, the extent of nuclear chromatin condensation could be correlated with changes in mitochondria structure. At 24 h after the addition of sulforaphane, the mitochondrial changes can be characterized with interruption and/or absence of the cristae and with loss of matrix density (Fig. 7E).

Expression of p53, bax, bcl-2, PARP, and Cytochrome c Proteins after Sulforaphane Treatment. To better determine which type of apoptotic pathway was induced by sulforaphane, extracts from HT29 cells at various times after sulforaphane treatment were examined by Western blotting using p53-, bax-, bcl-2-, PARP-, and cytochrome c-specific antibodies (Fig. 9). It is clear that HT29 cells do not undergo any change in p53 expression at any time point or sulforaphane concentration studied. By contrast, our results clearly show an increase in the bax protein content that appears after a 24-h period of treatment with 5 and 15 μ M sulforaphane, suggesting that sulforaphane induces apoptosis in HT29 cells via a bax-dependent pathway. The antiapoptotic protein bcl-2 was never detected under any conditions. We then examined whether the expression of bax could promote the release of mitochondrial cytochrome c into the cytosol. Fig. 9 also shows that as the level of bax increased, cytochrome c could be detected in the cytosol, whereas its level in the mitochondria decreased. Finally, the caspase cascade was also induced by sulforaphane, as shown by the proteolytic cleavage of PARP.

DISCUSSION

Many classes of cancer chemopreventive agents, including naturally occurring and pharmaceutical compounds, are studied for effi-

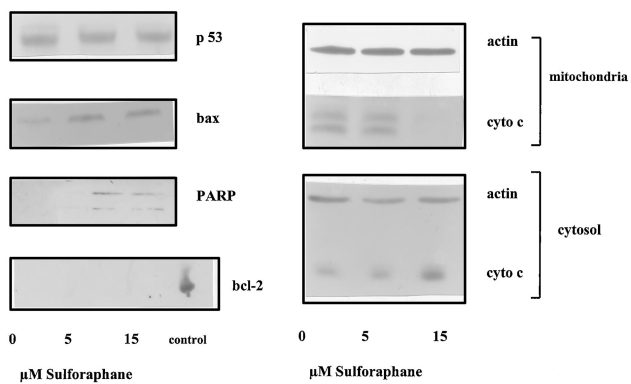


Fig. 9. Sulforaphane induces the expression of bax, the cleavage of PARP, and the release of cytochrome *c* but does not affect p53 or bcl-2 protein level. One day after seeding, HT29 cells were treated without (control cells) or with 5 or 15 μ M sulforaphane for 24 h. The whole cell extracts (2×10^5 cells) were used to measure the expression of bax, bcl-2, p53, and PARP by Western blotting. For the assay of cytochrome *c*, both cytosolic and mitochondrial fractions were prepared as described in "Materials and Methods." Cytochrome *c* and actin levels in cytosol and mitochondria were determined using Western blots. The unchanged level of actin in the different lanes ascertains equal loading. Polyacrylamide gels were prepared at 14% for bax and cytochrome *c* and at 7.5% for the p53 assay.

cacy *in vivo* and *in vitro*. Among the most extensively investigated are the isothiocyanates, which occur naturally in a variety of cruciferous vegetables such as cabbage (3, 4). Here we investigated whether sulforaphane, a member of the isothiocyanate family known to inhibit tumor development by activation of detoxifying enzymes, could alter carcinogenesis via other specific mechanisms. Our results clearly show for the first time that sulforaphane (10–30 μ M) induces cell cycle arrest and subsequent apoptotic death in the human colon cancer cell line HT29 in a dose-dependent manner. Necrotic or lytic effects were excluded by the lack of plasma membrane permeability as assessed by the absence of PI uptake or ATP release.

Apoptosis is a crucial element in the behavior of mammalian cells in many different situations (20). The apoptotic program is characterized by particular morphological features (21–24). In our model, we have clearly observed many of the typical structural and ultrastructural modifications that happen during the apoptotic pathway, which include cell shrinkage, translocation of PS to the outer layer of the plasma membrane, alteration of internal membrane of the mitochondria, and condensation of the cytoplasm or of nuclear chromatin. In contrast, we have never observed classical DNA fragmentation on sulforaphane treatment. This is not surprising because previous work (25) has shown that HT29 cells do not give rise to any of the DNA fragmentation patterns associated with programmed cell death when challenged with a variety of toxic stimuli.

Our results also clearly show that sulforaphane-induced HT29 cell death is not associated with a change in p53 protein expression but is accompanied by an overexpression of bax, one of the *bcl-2* gene family, acting as a promoter of cell death. In contrast, the antiapoptotic bcl-2 protein was not detected in our cells. bax is a protein present predominantly in the cytosol (26), which could partially translocate to the mitochondria on induction of apoptosis (27, 28). This induces the opening of the mitochondrial permeability transition pore, a critical event in the loss of cell viability that mediates the release of cytochrome *c*, finally activating the caspase cascade (28, 29). In our model (15 μ M sulforaphane), overexpression of the bax protein was correlated with cytochrome *c* release, suggesting it could trigger caspase-dependent apoptosis. This was evidenced by the presence of a proteolytic fragment of the caspase-3 substrate PARP in treated cells, suggesting that caspase-3 was activated, as has been recently shown in isothiocyanate-treated HeLa cells (30). Our con-

clusion is strengthened by the observation of abnormalities in the mitochondria ultrastructure identified by electron microscopy (Fig. 8) because altered mitochondrial functions have also been observed in other apoptotic colon cancer cells (31). Surprisingly, the high level of bax protein at 15 μ M sulforaphane was not associated with a high percentage of dead cells. However, the release of cytochrome *c* in the cytosol and the cleavage of PARP were also low at this concentration, suggesting a delay between the induction of bax and the final processes of apoptosis.

Due to the lipophilic nature of isothiocyanates, inhibition of phospholipid biosynthesis could have been a major event in the induction of growth arrest and apoptosis, as already reported for other lipidic compounds, *i.e.*, hexadecylphosphocholine (32), 1-O-octadecyl-2-*O*-methyl-rac-glycero-3-phosphocholine (33), or geranyl-geraniol (34). However, in our case, inhibition of phosphatidylcholine (the major class of phospholipid) biosynthesis was observed late (3 h) in contrast to DNA, RNA, or protein synthesis (10 min; Fig. 2), excluding an apoptosis related to phospholipid metabolism.

Because apoptosis is the end point of at least some colonic epithelial cell differentiation pathways, a process that results in apoptotic cell death should also minimize the proliferative signal. Indeed, in our model, apoptotic cell death is preceded by an arrest of the cell cycle and an accumulation of cells in G₂-M phase at the expense of S phase (Figs. 1 and 5). This is also evidenced by the increase in the level of cyclins B1 and A, proteins known to regulate cdc2 kinase activity at G₂-M phase (35). Because overexpression of bax has already been reported to induce the activation of cdk and caspase through the degradation of the cdk inhibitor P27 (36), it will be of interest to test whether the cdk inhibitors (p21, p27, and p16) are implicated in the negative regulation of cell cycle progression by sulforaphane in our model.

The resistance of cancer to therapy may be due in part to the high frequency of mutation in p53 that impairs p53-dependent apoptosis. Many anticancer agents such as doxorubicine, etoposide, or 5-fluorouracil induce apoptosis via a p53-dependent pathway (37). The requirement of p53 tumor suppressor for efficient activation of apoptosis by these agents provides an attractive explanation for the poor efficacy of these drugs on p53 mutant tumors (38). Thus, identifying chemotherapeutic agents that act independently of the p53 pathway is of major importance. Interestingly, the growth-inhibitory effect of sulforaphane was not apparently related to a change in p53 level. However, HT29 cells are known to present p53 mutations, and a strict p53-independent pathway in our model remains to be clearly demonstrated.

Although the presence of sulforaphane in the blood or intestine has not yet been quantified, consumption of 100 g of broccoli could release 40 μ mol of sulforaphane, suggesting that local concentrations in the low micromolar range may be achieved *in vivo* (39–41).

ACKNOWLEDGMENTS

We thank Cécile Vialat for technical assistance.

REFERENCES

- Steinmetz, K. A., and Potter, J. D. Vegetables, fruit and cancer. I. Epidemiology. *Cancer Causes Control*, 2: 325–357, 1991.
- Verhoeven, D. T. H., Verhagen, H., Goldbohm, R. A., van der Brandt, P. A., and van Poppel, G. A review of mechanisms underlying anticarcinogenicity by Brassica vegetables. *Chem. Biol. Interact.*, 103: 79–129, 1997.
- Hecht, S. S. Chemoprevention of cancer by isothiocyanates, modifiers of carcinogen metabolism. *J. Nutr.*, 129: 768S–774S, 1999.
- Talalay, P., and Zhang, Y. Chemoprevention against cancer by isothiocyanates and glucosinolates. *Biochem. Soc. Trans.*, 24: 806–810, 1996.
- Zhang, Y., and Talalay, P. Mechanism of differential potencies of isothiocyanates as inducers of anticarcinogenic phase 2 enzymes. *Cancer Res.*, 58: 4632–4639, 1998.

6. Prestera, T., and Talalay, P. Electrophile and antioxidant regulation of enzymes that detoxify carcinogens. *Proc. Natl. Acad. Sci. USA*, **92**: 8965–8969, 1995.
7. Stoner, G. D., Morrissey, D., Heur, H. Y., Daniel, E., Galati, A., and Wagner, S. A. Inhibitory effects of phenethylisothiocyanate on *N*-nitrosobenzylmethylamine carcinogenesis in the rat esophagus. *Cancer Res.*, **51**: 2063–2068, 1991.
8. Chen, Y. R., Wang, W., Kong, A. N. T., and Tan, T. H. Molecular mechanisms of c-Jun *N*-terminal kinase-mediated apoptosis induced by anticarcinogenic isothiocyanates. *J. Biol. Chem.*, **273**: 1769–1775, 1998.
9. Huang, C., Ma, W. Y., Li, J., Hecht, S. S., and Dong, Z. Essential role of p53 in phenethyl isothiocyanate-induced apoptosis. *Cancer Res.*, **58**: 4102–4106, 1998.
10. Zhang, Y., Kensler, T. W., Cho, C. G., Posner, G. H., and Talalay, P. Anticarcinogenic activities of sulforaphane and structurally related synthetic norbornyl isothiocyanates. *Proc. Natl. Acad. Sci. USA*, **91**: 3147–3150, 1994.
11. Faulkner, K., Mithen, R., and Williamson, G. Selective increase of the potential anticarcinogen 4-methylsulphinylbutyl glucosinolate in broccoli. *Carcinogenesis (Lond.)*, **19**: 605–609, 1998.
12. Barcelo, S., Gardiner, J. M., Gesher, A., and Chipman, J. K. CYP2E1-mediated mechanism of anti-genotoxicity of the broccoli constituent sulforaphane. *Carcinogenesis (Lond.)*, **17**: 277–282, 1996.
13. Gamet-Payastre, L., Lumeau, S., Gasc, N., Cassar, G., Rollin, P., and Tulliez, J. Selective cytostatic and cytotoxic effects of glucosinolates hydrolysis products on human colon cancer cells *in vitro*. *Anti-Cancer Drugs*, **9**: 141–148, 1998.
14. Schmid, H., and Karrer, P. Synthese der racemischen und der optisch aktiven formen des sulforaphans. *Helv. Chim. Acta*, **31**: 1497–1505, 1948.
15. Fogh, J., Fogh, J. N., and Orfeo, T. One hundred and twenty seven cultured human tumor cell lines producing tumors in nude mice. *J. Natl. Cancer Inst.*, **59**: 221–226, 1977.
16. Husoy, T., Syverson, T., and Jenssen, J. Comparison of four *in vitro* cytotoxicity tests: the MTT assay, NR assay, uridine incorporation and protein measurements. *Toxicol. In Vitro*, **7**: 149–154, 1993.
17. Vindelov, L. C., and Christensen, I. J. A review of techniques and results obtained in one laboratory by an integrated system of methods designed for routine clinical flow cytometric DNA analysis. *Cytometry*, **11**: 753–770, 1990.
18. Kamaryt, J., Muchova, M., and Stejska, J. Determination of adenosine phosphates in whole blood by capillary zone electrophoresis. *Eur. J. Clin. Chem. Clin. Biochem.*, **34**: 969–973, 1996.
19. Simm, A., Bertsch, G., Frank, H., Zimmermann, U., and Hoppe, J. Cell death of AKR-2B fibroblasts after serum removal: a process between apoptosis and necrosis. *J. Cell Sci.*, **110**: 819–828, 1997.
20. Jacobson, M. D., Weil, M., and Raff, M. C. Programmed cell death in animal development. *Cell*, **88**: 347–354, 1997.
21. Thompson, C. B. Apoptosis in the pathogenesis and treatment of disease. *Science (Washington DC)*, **267**: 1456–1461, 1995.
22. Tramp, B. F., Berezsky, I. K., Chang, S. H., and Phelps, P. C. The pathways of cell death: oncosis, apoptosis and necrosis. *Toxicol. Pathol.*, **25**: 82–88, 1997.
23. Goldsworthy, T. L., Connolly, R. B., and Fransson-Steen, R. Apoptosis and cancer risk assessment. *Mutat. Res.*, **365**: 71–90, 1996.
24. Stuart, M. C. A., Damoiseaux, J. G. M. C., Frederik, P. M., Arends, J. W., and Reuteulingsperger, C. P. M. Surface exposure of phosphatidylserine during apoptosis of rat thymocytes precedes nuclear changes. *Eur. J. Cell. Biol.*, **76**: 77–83, 1998.
25. Canman, C. E., Tang, T. Y., Normolle, D. P., Laurence, T. S., and Maybaum, J. Variations in patterns of DNA damage induced in human colorectal tumor cells by 5-fluorodeoxyuridine: implications for mechanisms of resistance and cytotoxicity. *Proc. Natl. Acad. Sci. USA*, **89**: 10474–10478, 1992.
26. Wolter, K. G., Hsu, Y. T., Smith, C. L., Nechushtan, A., Ki, X. G., and Youle, R. J. Movement of bax from the cytosol to mitochondria during apoptosis. *J. Cell. Biol.*, **139**: 1281–1292, 1997.
27. Pastorino, J. G., Chen, S. T., Tafani, M., Snyder, J. W., and Farber, J. L. The overexpression of bax produces cell death upon induction of the mitochondrial permeability transition. *J. Biol. Chem.*, **273**: 7770–7775, 1998.
28. Narita, M., Shimizu, S., Ito, T., Chittendens, T., Lutz, R. J., Matsuda, H., and Tsujimoto, Y. Bax interacts with the permeability transition pore to induce permeability transition and cytochrome *c* release in isolated mitochondria. *Proc. Natl. Acad. Sci. USA*, **95**: 14681–14686, 1998.
29. Granville, D. J., Carthy, C. M., Hunt, D. W. C., McManus, B. M. Apoptosis: molecular aspects of cell death and disease. *Lab. Investig.*, **78**: 893–913, 1998.
30. Yu, R., Mandelkar, S., Harvey, K. J., Ucker, D. S., and Kong, A. N. T. Chemopreventive isothiocyanates induce apoptosis and caspase-3-like protease activity. *Cancer Res.*, **58**: 402–408, 1998.
31. Mancini, M., Anderson, B. O., Caldwell, E., Sedghinasab, M., Paty, P. B., and Hockenberry, D. M. Mitochondrial proliferation and paradoxical membrane depolarization during terminal differentiation and apoptosis in a human colon carcinoma cell line. *J. Cell Biol.*, **138**: 449–469, 1997.
32. Boggs, K., Rock, C. O., and Jackowski, S. The antiproliferative effect of hexadecylphosphocholine toward HL60 cells is prevented by exogenous lysophosphatidylcholine. *Biochim. Biophys. Acta*, **1389**: 1–12, 1998.
33. Baburina, I., and Jackowski, S. Apoptosis triggered by 1-octadecyl-2-*O*-methyl-rac-glycero-3-phosphocholine is prevented by increased expression of CTP: phosphocholine cytidyltransferase. *J. Biol. Chem.*, **273**: 2169–2173, 1998.
34. Miquel, K., Pradines, A., Terce, A., Selmi, S., and Favre, G. Competitive inhibition of choline phosphotransferase by geranylgeraniol and farnesol inhibits phosphatidylcholine synthesis and induces apoptosis in human lung adenocarcinoma A549 cells. *J. Biol. Chem.*, **273**: 26179–26186, 1998.
35. Grana, X., and Reddy, E. P. Cell cycle control in mammalian cells: role of cyclins, cyclin dependent kinases (cdks) growth suppressor gene and cyclin-dependent kinase inhibitors (cdki). *Oncogene*, **11**: 211–219, 1995.
36. Gil-Gomez, G., Berns, A., and Brady, H. J. M. A link between cell cycle and cell death: Bax and bcl-2 modulate Cdk2 activation during thymocyte apoptosis. *EMBO J.*, **17**: 7209–7218, 1998.
37. Lowe, S. W., Ruley, H. E., Jacks, T., and Housman, D. E. p53 dependent apoptosis modulates the cytotoxicity of anticancer drugs. *Cell*, **74**: 957–967, 1993.
38. Fischer, D. E. Apoptosis in cancer therapy: crossing the threshold. *Cell*, **78**: 539–542, 1994.
39. Jiao, D., Yu, M., Hankin, J. H., Low, S. H., and Chung, F. L. Total isothiocyanates contents in cooked vegetables frequently consumed in Singapore. *J. Agric. Food Chem.*, **46**: 1055–1058, 1998.
40. Chiang, W. C. K., Pusateri, D. J., and Leitz, R. E. A. Gas chromatography/mass spectrometry method for the determination of sulforaphane and sulforaphanenitrile in broccoli. *J. Agric. Food Chem.*, **46**: 1018–1021, 1998.
41. Shapiro, T. A., Fahey, J. W., Wade, K. L., Stephensen, K. K., and Talalay, P. Human metabolism and excretion of cancer chemopreventive glucosinolates and isothiocyanates of cruciferous vegetables. *Cancer Epidemiol. Biomark. Prev.*, **7**: 1091–1100, 1998.